Journal of Hazardous Materials 172 (2009) 914–921

Contents lists available at ScienceDirect

Journal of Hazardous Materials

journal homepage: www.elsevier.com/locate/jhazmat

Photocatalytic activity of surface fluorinated TiO_2-P25 in the degradation of Reactive Orange 4

A. Vijayabalan, K. Selvam, R. Velmurugan, M. Swaminathan*

Department of Chemistry, Annamalai University, Annamalainagar 608002, India

ARTICLE INFO

Article history:
Received 20 February 2009
Received in revised form 16 July 2009
Accepted 21 July 2009
Available online 28 July 2009

Keywords:
Reactive Orange 4
Photocatalysis
Surface fluorination
TiO_2-P25
UV-A light
Hydrogen fluoride

ABSTRACT

Photocatalytic activity of surface fluorinated TiO_2-P25 (F-TiO_2-P25) in the degradation of a chlorotriazine azo dye Reactive Orange 4 (RO 4) under ambient conditions was investigated in this study. Characterization of F-TiO_2-P25 reveals that the catalyst has a strong absorption in the UV range and the presence of F atom in the catalyst. The degradation rate of RO 4 with surface fluorinated TiO_2-P25 is three times faster than bare TiO_2-P25. The quantum yield of UV/TiO_2-P25 process is largely decreased by the increase of initial dye concentration, whereas in UV/F-TiO_2-P25 process, the influence of initial dye concentration is less. Surface fluorination of TiO_2-P25 enhanced the adsorption of RO 4 dye, while improving overall degradation rate. The optimum operating conditions of UV/F-TiO_2-P25 process for efficient degradation are reported.

1. Introduction

In recent years, semiconductor photocatalytic technology has provided an effective and promising means for the destruction and mineralization of non-biodegradable organic pollutants in wastewater [1–4]. The photocatalyst used in this technology is mainly focused on TiO_2 due to its low cost, easy handling and environmental friendly features [5,6]. However, the activity of TiO_2 is not high enough for the requirements of practical applications [7]. Therefore increasing its photocatalytic activity is still a principal challenge in this research field. The introduction of new active sites into TiO_2 should be a feasible approach for improving the photocatalytic activity. A few researchers have reported the improvement of activity by surface fluorination of TiO_2 [8–11]. Surface fluorination can be done by a simple ligand exchange between surface hydroxyl groups on TiO_2 and fluoride ions.

$$\equiv \text{Ti–OH} + \text{F}^- \leftrightarrow \text{Ti-F} + \text{OH}^- \quad (1)$$

Minero et al. confirmed that fluoride enhanced the photodecomposition of phenol with TiO_2 in aqueous solutions and proposed that the fluorinated surface favored the generation of free OH radicals (not surface bound OH), which were responsible for the enhanced oxidation [12,13]. Kim and Choi not only confirmed this claim but also showed that hole mediated photocatalytic reactions were inhibited on the contrary because of the hindered adsorption of substrates on F-TiO_2 [14]. On the other hand, Lewandowski and Ollis [15] reported that the photocatalytic oxidation of aromatic air pollutants was unaffected for toluene or even inhibited for benzene or xylene by the surface fluorination of TiO_2. Judging from the results of previous studies, the effect of surface fluorination of TiO_2 could be either positive or negative depending on the kind of substrate and experimental conditions.

The Reactive Orange 4 (RO 4) dye (C.I. 18260, M.wt. 769.21) is extensively used in dyeing the textile fabrics. The chemical structure of RO 4 is shown in Fig. 1. The degradation of RO 4 using UV/TiO_2, UV/H_2O_2 and Fenton processes had been reported earlier from our laboratory [16–18]. During our study on surface modified photocatalysts we observed a 3-fold increase in the photoactivity of TiO_2-P25 by surface fluorination. Hence the main objective of this work was to study the effect of several parameters on the degradation of RO 4 by surface fluorinated TiO_2-P25 and to report the optimum conditions for efficient degradation. The reaction pathway of degradation is also discussed.

2. Experimental

2.1. Materials

Reactive Orange 4 (RO 4) (Colour Chem, Pondicherry) was used as received. A gift sample of TiO_2-P25 was obtained from Degussa (Germany). It has the particle size of 30 nm and BET specific sur-

* Corresponding author. Tel.: +91 4144 221670/220572; fax: +91 4144 220572.
E-mail address: chemres50@gmail.com (M. Swaminathan).

0304-3894/$ – see front matter © 2009 Published by Elsevier B.V.
doi:10.1016/j.jhazmat.2009.07.082

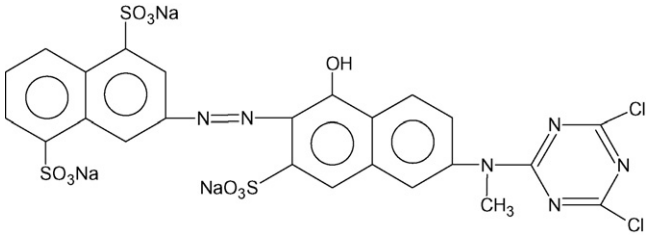

Fig. 1. Structure of Reactive Orange 4 dye.

face area of 55 $m^2\ g^{-1}$. AnalaR grade reagents H_2O_2 (30%, w/w), $(NH_4)_2S_2O_8$, $KBrO_3$, $KClO_3$, KIO_4, Na_2CO_3, Na_2SO_4, $NaHCO_3$ and $NaNO_3$ were used as received. The double distilled water was used to prepare experimental solutions. Hydrogen fluoride (HF) was used for fluorination. The pH before irradiation was adjusted using H_2SO_4 or NaOH. The natural pH of the aqueous solution is 4.8.

2.2. Irradiation experiments

All photochemical reactions were carried out under identical conditions using Heber photoreactor model HML-MP (Fig. 2). This model consists of eight medium pressure mercury vapor lamps (8 W) set in parallel and emitting 365 nm wavelength. It has a reaction chamber with specially designed reflectors made of highly polished aluminium and built in cooling fan at the bottom. It is provided with the magnetic stirrer at the center. Open borosilicate glass tube of 50 mL capacity, 40 cm height and 12.6 mm diameter was used as a reaction vessel. The irradiation was carried out using only four parallel medium pressure mercury lamps. The solution was aerated continuously by a pump to provide oxygen and for the complete mixing of solution. For the experiments using the F-TiO_2-P25, fluorination was achieved by adding appropriate concentration of HF, corresponding to the required amount of F^- per gram of TiO_2-P25. Fluoride ions are able to displace OH groups on the surface of TiO_2 very quickly [9]. Fluorinated catalyst (F-TiO_2-P25) was filtered and dried at room temperature. The catalyst was characterized by analytical methods. All solutions prior to photolysis were kept in dark by covering with aluminium foil to prevent any photochemical reactions.

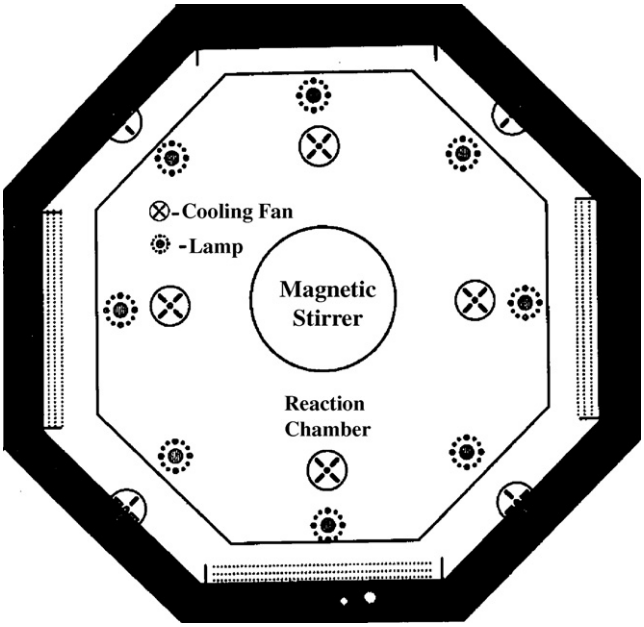

Fig. 2. Schematic diagram of photoreactor.

2.3. Analytical methods

Powder X-ray diffraction patterns of TiO_2 and F doped TiO_2 catalysts were obtained using a Philips PANanalytical X′ pert PRO diffractometer equipped with a Cu tube for generating a Cu Kα radiation (wavelength 1.5406 Å) at 40 kV, 25 mA. The particles were spread on a glass slide specimen holder and the scattered intensity was measured between 20° and 85° at a scanning rate of $2\theta = 1.2°\ min^{-1}$. Peak positions were compared with the standard files to identify the crystalline phases.

A Varian Cary 5E UV/VIS-NIR spectrophotometer equipped with an integrated sphere was used to record the diffuse reflectance spectra (DRS) and to measure the absorbance data of the samples. The baseline correction was performed using a calibrated reference sample of barium sulfate. The reflectance spectra of the F-TiO_2 catalysts were analyzed under ambient conditions in the wavelength range of 200–800 nm.

For FT-IR experiments, FT-IR spectrophotometer Thermo Nickolet was used. The samples were incorporated in KBr pellets for the measurements. Water reference spectrum was always subtracted from every spectrum.

2.4. Analysis

In all experiments 50 mL of reaction mixture was irradiated. At specific time intervals 1–2 mL of the sample was withdrawn and centrifuged to separate the catalyst. 1 mL centrifugate was suitably diluted and its absorbances at 489 and 285 nm were measured immediately. Its absorbance at 489 nm ($n \rightarrow \pi^*$ transition of –N=N– group) is due to the colour of dye solutions and it is used to monitor the decolourization of dye. The absorbance at 285 nm ($\pi \rightarrow \pi^*$ transition in naphthalene group) represents the aromatic content of RO 4 and the decrease at 285 nm indicates the degradation of aromatic part of dye. Since the decolourization is faster than degradation, the irradiation times of 10 min for decolourization and 30 min for degradation were chosen to compare the efficiencies. UV spectral measurements were made using Hitachi U-2001 spectrophotometer. The pH of the solution was measured using HANNA Phep (Model H 198107) digital pH meter.

2.5. GC–MS analysis

For identification of intermediate products of RO 4 photocatalytic degradation, the samples taken after 20 and 40 min were analyzed. The sample for analysis was prepared by the following method. The centrifugate obtained after irradiation was extracted five times with HPLC grade dichloromethane. The extract was dried over anhydrous sodium sulfate to remove the water present in the solution. The solvent was removed by evaporation under reduced pressure. The final residual mass was taken for GC–MS analysis.

3. Results and discussion

3.1. Characterization of fluorinated TiO_2-P25

The catalyst was characterized by PXRD, Diffuse Reflectance and FT-IR spectra. PXRD patterns were used to determine the crystalline forms and crystallinity of fluorinated TiO_2-P25 and bare TiO_2-P25 nanoparticles. Fig. 3 shows the XRD patterns of bare TiO_2-P25 and fluorinated TiO_2-P25 prepared with different concentrations of fluoride. The patterns reveal that all the samples are composed of both rutile and anatase phases. The fluorination has no obvious effects on the crystal structure of TiO_2. Moreover, the doping F atoms do not cause any shift in peak positions TiO_2-P25. This could be understood that the ion radius of fluorine atom (0.133 nm) is virtually the same as the replaced oxygen atom (0.132 nm) [19].

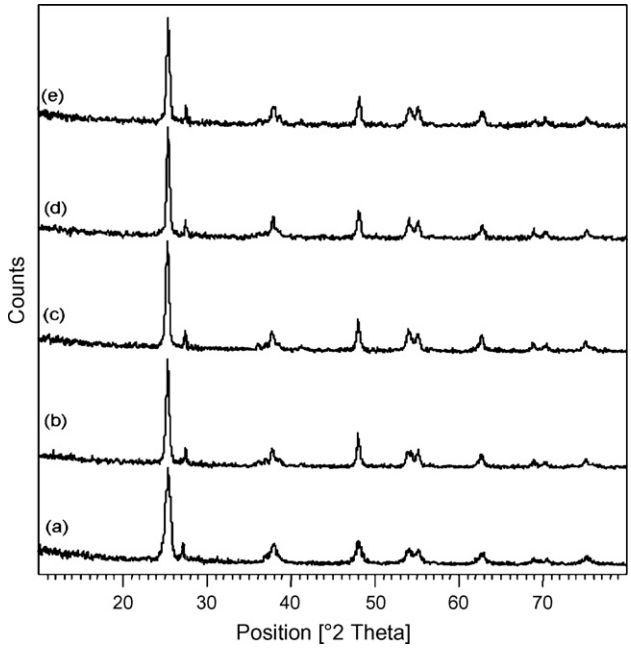

Fig. 3. XRD patterns of F-TiO_2-P25 and TiO_2-P25 nanoparticles: (a) Bare TiO_2-P25; (b) F-TiO_2-P25 (0.05 mmol F^-); (c) F-TiO_2-P25 (0.1 mmol F^-); (d) F-TiO_2-P25 (0.15 mmol F^-); (e) F-TiO_2-P25 (0.2 mmol F^-).

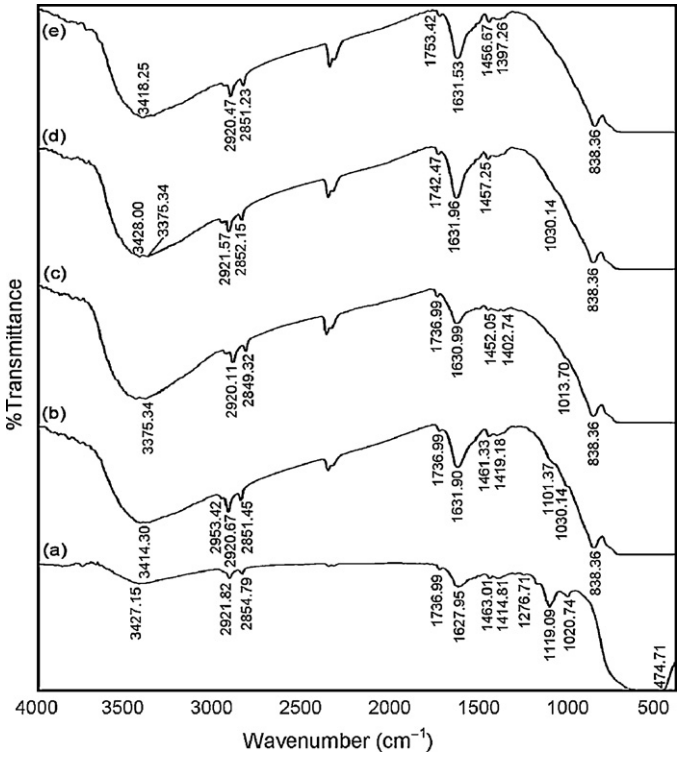

Fig. 5. FT-IR spectra of F-TiO_2-P25 and TiO_2-P25 nanoparticles: (a) Bare TiO_2-P25; (b) F-TiO_2-P25 (0.05 mmol F^-); (c) F-TiO_2-P25 (0.1 mmol F^-); (d) F-TiO_2-P25 (0.15 mmol F^-); (e) F-TiO_2-P25 (0.2 mmol F^-).

Diffuse reflectance spectra of the F-TiO_2-P25 samples are shown in Fig. 4. Fluorination clearly influenced the light absorption characteristics. Compared with the pure TiO_2-P25, the F-TiO_2-P25 samples showed a stronger absorption in the UV range and a slight shift to visible-light range (>430 nm). It has been reported that the F^- ion doping does not cause any shift in the fundamental absorption edge of TiO_2-P25 [20].

FT-IR spectra of the F-TiO_2-P25 catalysts are shown in Fig. 5. As reported in the literature, the small peak at 838.6 cm^{-1} is attributed to Ti–F vibration [21]. The intensities of other peaks increase by surface fluorination. The presence of Ti–F vibration peak indicated that F atoms were incorporated into the TiO_2 crystal lattice.

3.2. *Primary analysis of Reactive Orange 4 on fluorinated TiO_2-P25*

Photocatalytic degradation of Reactive Orange 4 (RO 4) with bare TiO_2-P25 and F-TiO_2-P25 at pH 3 was investigated and the results are presented in Fig. 6. It shows the influence of fluoride ion on the adsorption of RO 4 at pH 3. Prior to irradiation, the dispersions were magnetically stirred in the dark for 30 min to achieve the adsorption–desorption equilibrium between TiO_2-P25 and RO 4. The pre-adsorption measurements showed that about 12% of RO 4 was adsorbed on naked TiO_2-P25 surface. The presence of 0.2 mmol fluoride ion increased the adsorption of RO 4 to 30%.

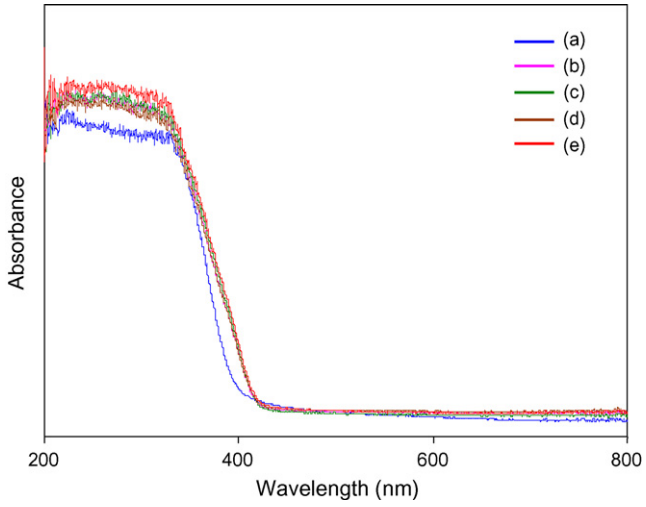

Fig. 4. DRS spectra of F-TiO_2-P25 and TiO_2-P25 nanoparticles: (a) Bare TiO_2-P25; (b) F-TiO_2-P25 (0.05 mmol F^-); (c) F-TiO_2-P25 (0.1 mmol F^-); (d) F-TiO_2-P25 (0.15 mmol F^-); (e) F-TiO_2-P25 (0.2 mmol F^-).

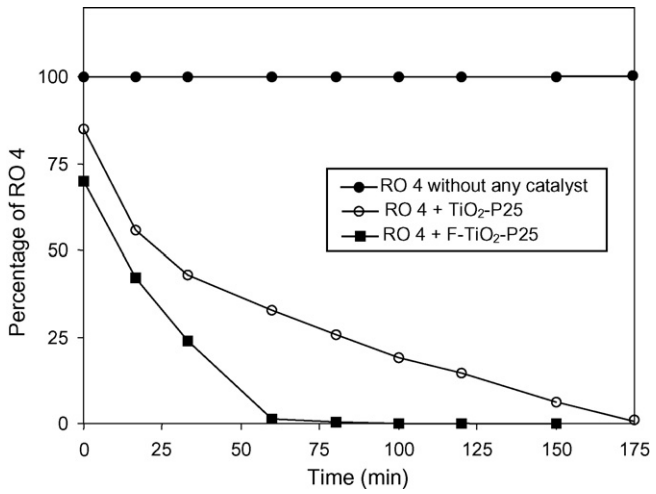

Fig. 6. Photodegradability and adsorption of F-TiO_2-P25: [RO 4] = 5×10^{-4} mol L^{-1}; pH = 3 ± 0.1; catalyst suspended = 4 g L^{-1}; fluoride ion = 0.2 mmol; airflow rate = 8.1 mL s^{-1}; $I = 1.381 \times 10^{-3}$ Einstein L^{-1} s^{-1}.

It is observed that the RO 4 degradation rate proceeds much more rapidly in the presence of F-TiO_2-P25 and the degradation rate of RO 4 is up to three times higher than that in the absence of fluoride ions. The complete degradation of RO 4 is achieved at 60 min of irradiation with F-TiO_2-P25 whereas in bare TiO_2-P25, the complete mineralization occurs at the time of 175 min irradiation. Both degradations can be fitted reasonably well by an exponential decay curve suggesting a first order kinetics. The resulting first order rate constant k_{app} has been used to calculate the quantum yield.

The efficiency of the photocatalytic degradation has been analyzed using the quantum yield. The quantum yield of a reaction is defined as the number of RO 4 molecules being decomposed (degraded) per photon absorbed (Eq. (2)).

$$\Phi = \frac{\text{number of molecules decomposed}}{\text{number of photons of light absorbed}} \quad (2)$$

The photodegradation rate constant (k') of RO 4 under the monochromatic light source can also be used for the calculation of its reaction quantum yield using Eq. (3) [22]

$$\Phi = \frac{k'}{2.303 I_{0,\lambda} \varepsilon_{D,\lambda} l} \quad (3)$$

where Φ is the reaction quantum yield (dimensionless), $I_{0,\lambda}$ is the intensity of the incident light at 365 nm (1.38×10^{-6} Einstein L^{-1} s^{-1}), $\varepsilon_{D,\lambda}$ is the molar absorptivity of RO 4 at 365 nm, and l is the path length of reaction tube. The molar absorptivity ε was determined from the absorbance of RO 4 at 365 nm (2.36×10^{-4} M). Since the emission of the lamp is maximum at 365 nm, the intensity at this wavelength was used for calculation. Furthermore the same intensity was used for the calculation of quantum yield for all the samples containing RO 4. The quantum yields of the photodegradation of RO 4 with F-TiO_2-P25 and TiO_2-P25 were determined to be 0.703 and 0.207, respectively. About 3.5 times enhancement in photocatalytic degradation of RO 4 with F-TiO_2-P25 is observed under these conditions. According to Minero et al. [12], the preferential formation of free OH radicals on F-TiO_2-P25 (Eqs. (4) and (5)) should be responsible for this fluoride enhanced photocatalytic activity:

$$h_{vb}^{+} + H_2O_{ad} \rightarrow H_2O^{\bullet +} \text{ (on F-TiO}_2\text{-P25)} \quad (4)$$

$$H_2O^{\bullet +} \rightarrow H^{+} + OH_{free}^{\bullet} \text{ (on F-TiO}_2\text{-P25)} \quad (5)$$

$$h_{vb}^{+} + \text{Ti–OH}_{surf} \rightarrow \text{Ti-OH}_{surf}^{\bullet} \text{ (on naked – TiO}_2\text{-P25)} \quad (6)$$

The photocatalytic degradation occurs mainly on the solution phase by hydroxyl radicals. The oxidizing power of hydroxyl radicals produced by these catalysts is strong enough to break C–C, C–H, C=C bonds of RO 4 adsorbed on their surfaces leading to the formation of CO_2 and mineral acids. Passing the evolved gas during the experiment in to lime water has been used for testing CO_2 formation. The formation of CO_2 was further confirmed by the precipitation of $BaCO_3$, when the evolved gas was passed through concentrated $Ba(OH)_2$ solution.

3.3. Effect of fluoride and catalyst concentrations

To investigate the optimum fluoride concentration for efficient photocatalytic degradation, the amount of fluoride concentration was varied between 0.05 and 0.5 mmol in a series of experiments at constant process conditions: TiO_2-P25 = 4 g L^{-1}, dye concentration = 5×10^{-4} M, solution pH 3, incident photon flux (I) = 1.381×10^{-6} Einstein L^{-1} s^{-1}, airflow rate = 8.1 mL s^{-1}. The results are illustrated in Fig. 7. The rate constant for the degradation increases from 0.020 to 0.045 min^{-1} with the increase of fluoride concentration from 0.05 to 0.2 mmol at the time of 30 min irradiation. Further increase of fluoride concentration from 0.2 to 0.5 mmol decreases rate constant from 0.045 to 0.030 min^{-1}. Hence under these experimental conditions 0.2 mmol of fluoride ion is found to be optimum for efficient removal of RO 4. The catalyst prepared with 0.2 mmol of fluoride ion was used in all the experiments.

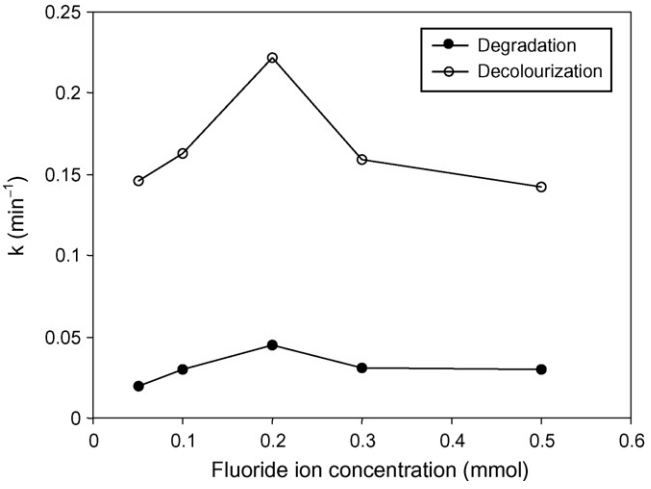

Fig. 7. Effect of fluoride concentrations: [RO 4] = 5×10^{-4} mol L^{-1}; pH = 3 ± 0.1; catalyst suspended = 4 g L^{-1}; airflow rate = 8.1 mL s^{-1}; I = 1.381×10^{-3} Einstein L^{-1} s^{-1}.

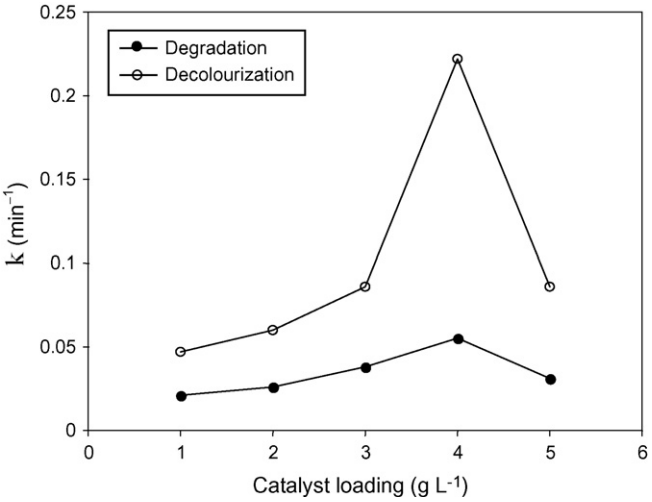

Fig. 8. Effect of catalyst concentrations: [RO 4] = 5×10^{-4} mol L^{-1}; pH = 3 ± 0.1; airflow rate = 8.1 mL s^{-1}; I = 1.381×10^{-3} Einstein L^{-1} s^{-1}.

Fig. 8 shows first order rate constants for different concentrations of catalyst. The increase of F-TiO_2-P25 concentration from 1 to 4 g L^{-1} increases the rate constant from 0.021 to 0.045 min^{-1}. Further increase of catalyst concentration from 4 to 5 g L^{-1} decreases the rate constant from 0.045 to 0.031 min^{-1}. At a lower concentration range, increase of catalyst concentration provides more reactive sites resulting in the enhancement of degradation rate. At a higher dye concentration range, the solution becomes cloudy and opaque. This reduces light penetration leading to the reduction of availability of active sites. The increase in concentration of catalyst may also result in the aggregation of free catalyst particle causing opacity of the solution. Hence the optimum concentration of catalyst (F-TiO_2-P25) is 4 g L^{-1}.

3.4. Effect of solution pH

In order to realize the effect of pH on the photocatalytic degradation of RO 4 by F-TiO_2-P25, photocatalytic degradation of RO 4

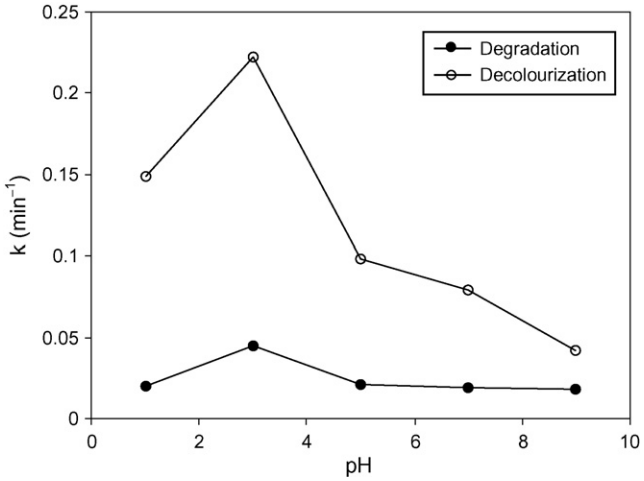

Fig. 9. Effect of solution pH: [RO 4] = 5×10^{-4} mol L^{-1}; F-TiO_2-P25 = 4 g L^{-1}; airflow rate = 8.1 mL s^{-1}; $I = 1.381 \times 10^{-3}$ Einstein L^{-1} s^{-1}.

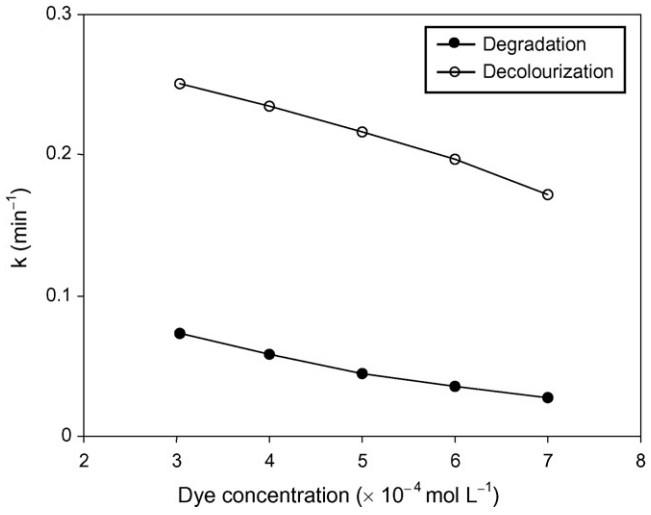

Fig. 10. Effect of various initial dye concentrations: pH = 3 ± 0.1; F-TiO_2-P25 = 4 g L^{-1}; airflow rate = 8.1 mL s^{-1}; $I = 1.381 \times 10^{-3}$ Einstein L^{-1} s^{-1}.

on the catalyst was performed at different pH values. The pH of the solution was adjusted before irradiation and it was not controlled during the reaction. The results are presented in Fig. 9. It can be seen that the degradation rate constant values of RO 4 are 0.020, 0.045, 0.021, 0.019 and 0.018 min^{-1} and decolourization values are 0.149, 0.222, 0.098, 0.079 and 0.042 min^{-1} at pH 1, 3, 5, 7 and 9, respectively. The effect of pH on the degradation rate is remarkable in our experimental conditions. The degradation rate at acidic condition is larger than that at alkaline condition.

It was difficult to elucidate clearly the effect of pH on photocatalytic process. An inner F-TiO_2-P25 complex is formed by the replacement of surface hydroxyl groups. Therefore the adsorption of the electronegative organic anionic compound is usually suppressed [23]. However, the existence of fluoride ion partially neutralizes the positive charge on the surface of TiO_2-P25. RO 4 dye molecules are adsorbed on the surface of TiO_2-P25 through an electrostatic interaction between fluoride ion and dye molecules. An experiment to verify the dark adsorption of RO 4 under different pH was carried out. The percentages of adsorption at pH 3, 5, 7 and 9 are found to be 76.11, 72.61, 62.61 and 49.66 after the attainment of adsorption–desorption equilibrium. Since the adsorption is high at pH 3, the degradation is also efficient at this pH. This reveals that the adsorption of RO 4 plays a vital role in the degradation mechanism.

It is well known that the surface of TiO_2-P25 is readily hydroxylated in aqueous solution. There are three kinds of surface species $TiOH_2^+$, TiOH, TiO^-, whose proportion depend on solution pH and point of zero charge (Pzc) of TiO_2. The Pzc for TiO_2-P25 is ≈6.8 [24]. When pH is less than Pzc, i.e., at pH 3, TiO_2-P25 surface is positively charged (Eq. (7)).

$$\text{When pH} < \text{Pzc}: \quad \text{TiOH} + \text{H}^+ \leftrightarrow \text{TiOH}_2^+ \tag{7}$$

In case of fluorinated TiO_2-P25, the species TiOH is replaced by TiF. So at pH 3 the TiF will be positively charged by Eq. (8).

$$\text{TiF} + \text{H}^+ \leftrightarrow \text{TiFH}^+ \tag{8}$$

Since RO 4 contains three sulfonated groups, the hydrolysed molecule behaves as a trianionic dye at pH 3 and more dye is adsorbed on F-TiO_2-P25 due to the electrostatic attraction between $TiFH^+$ and anionic dye molecules.

3.5. Effect of substrate concentration

The effect of various initial dye concentrations on the rate of dye degradation of RO 4 was performed by varying dye concentration from 3 to 7 × 10^{-4} mol L^{-1} with constant catalyst loading at pH 3 and the results are shown in Fig. 10. The increase of substrate concentration from 3 to 7 × 10^{-4} mol L^{-1} decreases the rate constant from 0.073 to 0.027 for degradation in 30 min and 0.249 to 0.168 for decolourization in 10 min.

Table 1
The quantum yield of dye degradation with F-TiO_2-P25 and bare TiO_2-P25 at various initial dye concentrations of RO 4.

Dye concentrations ($\times 10^{-4}$ M)	Quantum yield, Φ	
	TiO_2-P25	F-TiO_2-P25
3	0.6026	0.9227
4	0.4773	0.8299
5	0.2133	0.7530
6	0.1380	0.7056
7	0.0987	0.6661

pH = 3 ± 0.1, catalyst suspended = 4 g L^{-1}, airflow rate = 8.1 mL s^{-1}, $I = 1.381 \times 10^{-3}$ Einstein L^{-1} s^{-1}, irradiation time = 30 min.

At high dye concentration a significant amount of UV light of 365 nm may be absorbed by dye molecules and this reduces the absorbance of UV-A light by the catalyst. The increase in dye concentration also decreases the path length of photon entering this solution. It should be pointed out that even at high initial concentration of RO 4 (7 × 10^{-4} mol L^{-1}) about 55.63% dye removal could be achieved in 30 min. This indicates that F-TiO_2-P25 catalyst can also work well at a high initial concentration of RO 4.

The quantum yields for degradation for UV/F-TiO_2-P25 and UV/TiO_2-P25 processes at various initial dye concentrations of RO 4 are given in Table 1. When the dye concentration increases from 3 to 7 × 10^{-4} mol L^{-1}, the quantum yield decreases by 6.10- and 1.38-fold in UV/TiO_2-P25 and UV/F-TiO_2-P25 processes, respectively. The results indicate that the quantum yield of UV/TiO_2-P25 process is heavily influenced by the initial dye concentration, whereas the UV/F-TiO_2-P25 process is less affected by initial dye concentration. Another interesting result is noticed in these two processes at low and high initial dye concentrations. At low initial concentration (3 × 10^{-4} mol L^{-1}) the quantum yield of UV/F-TiO_2-P25 process (Φ = 0.9227) is 1.53-fold more efficient than UV/TiO_2-P25 process (Φ = 0.6026). But at high initial concentration (7 × 10^{-4} mol L^{-1}) UV/F-TiO_2-P25 (Φ = 0.6661) is 6.7-fold more efficient than UV/TiO_2-P25 (Φ = 0.0987) process. This reveals that F-TiO_2-P25 catalyst is more suitable at high initial dye concentration than TiO_2-P25 for the degradation of RO 4.

Table 2
Effect of oxidants on photodegradation of RO 4 with F-TiO_2-P25.

Oxidants	Degradation (%)	Quantum yield, Φ
F-TiO_2-P25	74.21	0.753
KIO_4	89.47	1.254
$KBrO_3$	85.54	0.945
$(NH_4)_2S_2O_8$	77.46	1.113
$KClO_3$	75.46	0.865
H_2O_2	82.14	1.054

[RO 4] = 5×10^{-4} mol L^{-1}, pH = 3 ± 0.1, catalyst suspended = 4 g L^{-1}, airflow rate = 8.1 mL s^{-1}, $I = 1.381 \times 10^{-3}$ Einstein L^{-1} s^{-1}, oxidants = 0.01 M, irradiation time = 30 min.

3.6. Other factors influencing photodegradation of RO 4 with F-TiO_2-P25

The influence of various factors on degradation of RO 4 with F-TiO_2-P25 was examined with optimized conditions ([RO 4] = 5×10^{-4} M; F-TiO_2-P25 = 4 g L^{-1}; airflow rate = 8.1 mL s^{-1}; pH 3; $I = 1.381 \times 10^{-5}$ Einstein L^{-1} s^{-1}). The effect of oxidants such as KIO_4, $(NH_4)_2S_2O_8$, $KClO_3$, $KBrO_3$ and H_2O_2 in addition to molecular oxygen on the degradation kinetics of the employed model compound was investigated. It was found that addition of these oxidants enhances the photodegradation of RO 4 (Table 2). The higher degree of degradation in this process with the oxidants is due to formation of highly reactive radical intermediates and the electron capture by these oxidants (Eqs. (9)–(16)) [25].

$$IO_4^{\bullet -} + h\nu \rightarrow IO_3^{\bullet} + O^{\bullet -} \quad (9)$$

$$O^{\bullet -} + H^+ \rightarrow {}^{\bullet}OH \quad (10)$$

$$H_2O_2 \xrightarrow{h\nu} {}^{\bullet}OH \quad (11)$$

$$S_2O_8^{2-} \xrightarrow{h\nu} 2SO_4^{\bullet -} \quad (12)$$

$$SO_4^{\bullet -} + H_2O \rightarrow {}^{\bullet}OH + SO_4^{2-} + H^+ \quad (13)$$

$$S_2O_8^{2-} + e_{CB}^- \rightarrow SO_4^{\bullet -} + SO_4^{2-} \quad (14)$$

$$BrO_3^- + 6e_{CB}^- + 6H^+ \rightarrow Br^- + 3H_2O \quad (15)$$

$$ClO_3^- + 6e_{CB}^- + 6H^+ \rightarrow ClO_2^- + H_2O_2 \quad (16)$$

The respective one electron reduction potentials of different species are E ($O_2/O_2^{\bullet -}$) = −115 mV, E ($H_2O_2/{}^{\bullet}OH$) = 800 mV, E ($BrO_3^-/BrO_2^{\bullet}$) = 1150 mV and E ($S_2O_8^{2-}/SO_4^{2-}$) = 1100 or 2123 mV [26]. From the thermodynamic point of view all employed additives should therefore be more efficient electron acceptors than molecular oxygen. Hence, they act as the strong oxidants and electron acceptors inhibiting the electron-hole recombination.

Since a number of auxiliary chemicals are added in the dyeing process, the effluent contains inorganic ions such as carbonate, sulfate, etc. Hence it is important to study the influence of these ions in the photodegradation. Table 3 gives the results on the effect of added inorganic anions like carbonate, bicarbonate, sulfate and nitrate of sodium salts at pH 3. In the illuminated TiO_2-P25 system 25.78, 41.41, 71.00 and 84.78% of degradations were observed

Table 3
Effect of anions on photodegradation of RO 4 with F-TiO_2-P25.

Anions	Degradation (%)	Quantum yield (Φ)
F-TiO_2-P25	74.21	0.753
$NaNO_3$	71.00	0.704
Na_2SO_4	84.78	0.801
$NaHCO_3$	41.41	0.423
Na_2CO_3	25.78	0.214

[RO 4] = 5×10^{-4} mol L^{-1}, pH = 3 ± 0.1, catalyst suspended = 4 g L^{-1}, airflow rate = 8.1 mL s^{-1}, $I = 1.381 \times 10^{-3}$ Einstein L^{-1} s^{-1}, anions = 0.01 M, irradiation time = 30 min.

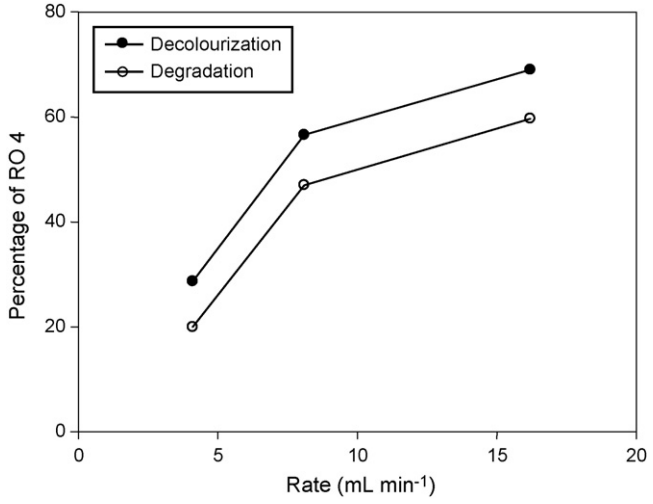

Fig. 11. Effect of airflow rate on degradation of RO 4: [RO 4] = 5×10^{-4} mol L^{-1}; pH = 3 ± 0.1; F-TiO_2-P25 = 4 g L^{-1}; $I = 1.381 \times 10^{-3}$ Einstein L^{-1} s^{-1}.

with Na_2CO_3, $NaHCO_3$, $NaNO_3$ and Na_2SO_4, respectively for 30 min irradiation at pH 3. The main inhibition effect is due to their adsorption on TiO_2 surface [27]. As can be seen from the values (Table 2) the degradation efficiency of UV/F-TiO_2-P25 was significantly decreased in the presence of CO_3^{2-}, HCO_3^- whereas the efficiency increased in the presence of SO_4^{2-}. The SO_4^{2-} ion may form sulfate radical anion ($SO_4^{\bullet -}$) which can accelerate the reaction (Eq. (14)). No significant change was observed for NO_3^- ion. Addition of CO_3^{2-}, HCO_3^-, ions decreases degradation of RO 4 due to the hydroxyl radical quenching by these ions. The order of inhibition of these anions is $CO_3^{2-} > HCO_3^- > NO_3^-$.

Study of photodegradation at different airflow rates reveals enhancement of degradation rate with the increase in flow rate (Fig. 11). The increase of airflow rate from 4.1 to 8.1 mL s^{-1} increases the degradation sharply from 27 to 58% in 30 min. For further increase of airflow rate from 8.1 to 16.2 mL s^{-1}, the enhancement is gradual.

3.7. Proposed mechanism of degradation

To find out the mechanism of highly efficient photodegradation of F-TiO_2-P25, iodide ion oxidation experiments by TiO_2-P25 photocatalysis with and without surface fluorination were carried out. Ishibashi et al. once estimated the quantum yield of photogenerated holes simply by iodide ion photocatalytic oxidation [28]. It is well known that I^- is very easily oxidized by the holes formed from photoexcited TiO_2-P25 to produce I_2. Therefore, the yield of holes can be determined by estimating the produced I_2. Irradiation of 0.1 M of KI with TiO_2-P25 and F-TiO_2-P25 under the same conditions, with UV-A light for 60 min shows higher iodine generation for F-TiO_2-P25 (Fig. 12). The iodine formed was found from the absorbance spectra of the illuminated solution. This iodide ion oxidation revealed that the concentration of iodine formed in the presence of F-TiO_2-P25 is up to three times of that in the presence of bare TiO_2-P25. This indicates that surface fluorination promotes the hole availability. When the TiO_2-P25 surface was modified by fluoride ion, more holes were available and subsequently more hydroxyl radicals were generated. As a result, the photocatalytic degradation is enhanced by fluorination (Eqs. (17) and (18)).

$$\equiv Ti\text{–}F + H_2O + h_{vb}^+ \rightarrow \equiv Ti\text{–}F + {}^{\bullet}OH_{free\,(aq)} + H^+ \quad (17)$$

$$RO\,4 + {}^{\bullet}OH \rightarrow CO_2 + H_2O + \text{mineralacids} \quad (18)$$

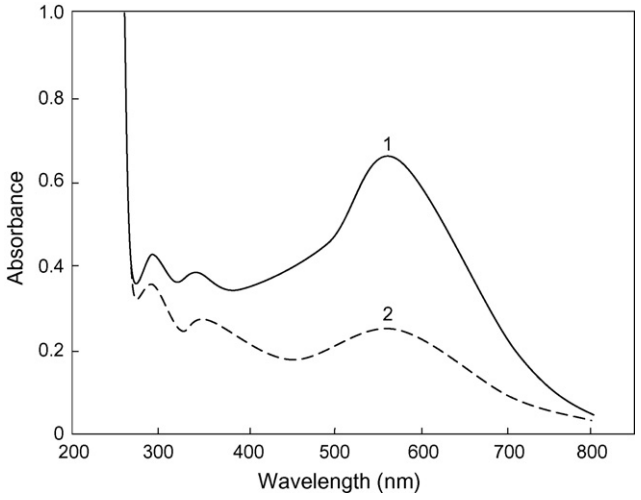

Fig. 12. Oxidation of I^- in aqueous suspension with: (1) F-TiO_2-P25; (2) TiO_2-P25.

3.8. Photodegradation pathway

An attempt was made to identify the intermediate products formed in the photocatalytic degradation of the dye through GC–MS analysis. The GC–MS analysis of solution after 20 and 40 min irradiation showed the formation of one main product with the retention time of 12.73. This product was identified by the molecular ion and mass spectrometric fragmentation peaks (compound **2**: 304–150, 136, 123, 109, 95, 83, 67, 52).

The formation of this compound from the photoreaction of dye molecule is shown in Scheme 1. The attack of hydroxyl radical on the carbons bearing azo linkage and sulphonate groups leads to the formation of a trihydroxy compound **1** and this on dehydroxylation and protonation gives **2**, in which a naphthalene ring is linked to a triazine system through $-N(CH_3)-$ linkage. This compound on further irradiation is mineralized. After 60 min of irradiation the mineralization of the dye is almost complete. The formation of CO_2, NO_3^-, SO_4^{2-} were identified by the usual procedure.

3.9. Mineralization studies

The mineralization of RO 4 was also studied by COD measurements in F-TiO_2-P25 system (Table 4). The COD measurements reveal that the COD of 2792 mg/L of the initial dye concentration of 5×10^{-4} mol L^{-1}gradually decreases with increasing irradiation period under optimum conditions with F-TiO_2-P25. After 60 min irradiation, the COD value of 270 mg L^{-1} indicates that RO 4 has

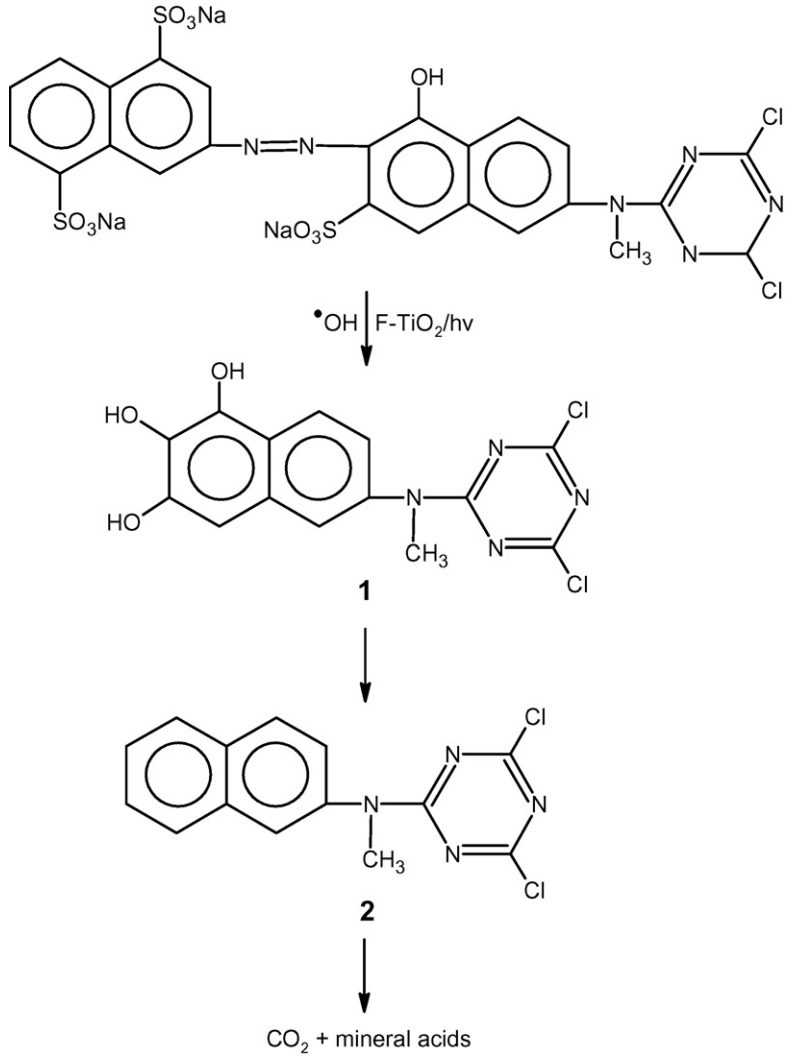

Scheme 1.

Table 4
COD analysis of RO 4 with F-TiO_2-P25 at different times of irradiation.

Time	COD (mg/L)
0 min	2792
20 min	1441
40 min	900
60 min	270

[RO 4] = 5×10^{-4} mol L^{-1}, pH = 3 ± 0.1, catalyst suspended = 4 g L^{-1}, airflow rate = 8.1 mL s^{-1}, $I = 1.381 \times 10^{-3}$ Einstein L^{-1} s^{-1}.

been degraded by 90% which is very close to complete mineralization.

4. Conclusions

This study clearly demonstrated that the surface fluorination of TiO_2-P25 enhances the photocatalytic activity. The efficiency of RO 4 degradation increases with increase in the fluoride concentration up to 0.2 mmol and then decreases. Diffuse reflectance spectrum of F-TiO_2-P25 indicates that the catalyst has a strong absorption in the UV range which is slightly extended to the visible region. The presence of F atoms in the catalyst is revealed by FT-IR spectrum. The optimum F-TiO_2-P25 loading and pH are found to be 4 g L^{-1} and 3. Surface fluorination enhanced the adsorption of RO 4 dye while improving overall degradation rate. The quantum yield of UV/F-TiO_2-P25 process is less affected by initial dye concentration. The addition of oxidants significantly enhances the UV/F-TiO_2-P25 process. Efficiency of F-TiO_2-P25 decreases in the presence of CO_3^{2-}, HCO_3^- but increases in the presence of SO_4^{2-}. The enhancement of photocatalytic degradation of RO 4 by F-TiO_2-P25 is mainly due to higher generation of hydroxyl radicals by more available holes in F-TiO_2-P25 as evidenced by iodide ion oxidation. Under these conditions this surface fluorinated TiO_2-P25 can be efficiently applied for the treatment of dye industrial effluent with higher dye concentrations.

Acknowledgement

One of the authors, K. Selvam is thankful to CSIR, New Delhi, for the award of Senior Research Fellowship.

References

[1] M.R. Hoffmann, S.T. Martin, W. Choi, D.W. Bahnemann, Environmental applications of semiconductor photocatalysis, Chem. Rev. 95 (1995) 69–96.
[2] R.W. Matthews, S.R. McEvoy, Photocatalytic degradation of phenol in the presence of near-UV illuminated titanium dioxide, J. Photochem. Photobiol. A 64 (1992) 231–246.
[3] H. Gerischer, Photoelectrochemical catalysis of the oxidation of organic molecules by oxygen on small semiconductor particles with TiO_2 as an example, Electrochim. Acta 38 (1993) 3–9.
[4] O. Legrini, E. Oliveros, A.M. Braun, Photochemical processes for water treatment, Chem. Rev. 93 (1993) 671–698.
[5] D.W. Bahnemann, in: E. Pelizzeti, M. Schiavello (Eds.), Mechanisms of Organic Transformations on Semiconductor Particle, Kluwer Academic Publishers, Netherlands, 1991, p. 251.
[6] S. Sakthivel, M.V. Shankar, M. Palanichamy, B. Arabindoo, V. Murugesan, Photocatalytic decomposition of leather dye: comparative study of TiO_2 supported on alumina and glass beads, J. Photochem. Photobiol. A 148 (2002) 153–159.
[7] D.Y. Goswami, A review of engineering developments of aqueous phase solar photocatalytic detoxification and disinfection processes, J. Sol. Energy Eng. 119 (1997) 101–107.
[8] H. Park, W. Choi, Effects of TiO_2 surface fluorination on photocatalytic reactions and photoelectrochemical behaviors, J. Phys. Chem. B 108 (2004) 4086–4093.
[9] J.S. Park, W. Choi, Enhanced remote photocatalytic oxidation on surface-fluorinated TiO_2, Langmuir 20 (2004) 11523–11527.
[10] J.S. Park, W. Choi, Remote photocatalytic oxidation mediated by active oxygen species penetrating and diffusing through polymer membrane over surface fluorinated TiO_2, Chem. Lett. 34 (2005) 1630–1632.
[11] J. Ryu, W. Choi, Effects of TiO_2 surface modifications on photocatalytic oxidation of arsenite: the role of superoxides, Environ. Sci. Technol. 38 (2004) 2928–2933.
[12] C. Minero, G. Mariella, V. Maurino, E. Pelizzetti, Photocatalytic transformation of organic compounds in the presence of inorganic anions. 1. Hydroxyl-mediated and direct electron-transfer reactions of phenol on a titanium dioxide–fluoride system, Langmuir 16 (2000) 2632–2641.
[13] C. Minero, G. Mariella, V. Maurino, D. Vione, E. Pelizzetti, Photocatalytic transformation of organic compounds in the presence of inorganic ions. 2. Competitive reactions of phenol and alcohols of a titanium dioxide–fluoride system, Langmuir 16 (2000) 8964–8972.
[14] H. Kim, W. Choi, Effects of surface fluorination of TiO_2 on photocatalytic oxidation of gaseous acetaldehyde, Appl. Catal. B 69 (2007) 127–132.
[15] M. Lewandowski, D.F. Ollis, Halide acid pretreatments of photocatalysts for oxidation of aromatic air contaminant: rate enhancement, rate inhibition, and a thermodynamic rationale, J. Catal. 217 (2003) 38–46.
[16] M. Muruganandham, M. Swaminathan, Solar photocatalytic degradation of a reactive azo dye in TiO_2-suspension, Sol. Energy Mater. Sol. Cells 81 (2004) 439–457.
[17] M. Muruganandham, M. Swaminathan, Photochemical oxidation of reactive azo dye with UV-H_2O_2 process, Dyes Pigments 62 (2004) 269–275.
[18] M. Muruganandham, M. Swaminathan, Decolourisation of Reactive Orange 4 by Fenton and photo-Fenton oxidation technology, Dyes Pigments 63 (2004) 315–321.
[19] D. Li, H. Haneda, S. Hishita, N. Ohashi, N.K. Labhsetwar, Fluorine-doped TiO_2 powders prepared by spray pyrolysis and their improved photocatalytic activity for decomposition of gas-phase acetaldehyde, J. Fluorine Chem. 126 (2005) 69–77.
[20] W. Ho, C.Y. Yu, S. Lee, Synthesis of hierarchical nanoporous F-doped TiO_2, spheres with visible light photocatalytic activity, Chem. Commun. (2006) 1115–1117.
[21] J.C. Yu, J.G. Yu, W.K. Ho, Z.T. Jiang, L.Z. Zhang, Effects of F^- doping on the photocatalytic activity and microstructures of nanocrystalline TiO_2 powders, Chem. Mater. 14 (2002) 3808.
[22] W. Chu, Modeling the quantum yields of herbicide 2,4-D decay in UV/H_2O_2 process, Chemosphere 44 (2001) 935–941.
[23] Y. Chen, S. Yang, K. Wang, L. Lou, Role of primary active species and TiO_2 surface characteristic in UV-illuminated photodegradation of acid Orange 7, J. Photochem. Photobiol. A 172 (2005) 47–54.
[24] I.A. Alaton, I.A. Balcioglu, D.W. Bahnemann, Advanced oxidation of a reactive dyebath effluent: comparison of O_3, H_2O_2/UV-C and TiO_2/UV-A processes, Water Res. 36 (2002) 1143–1154.
[25] E. Evgenidou, K. Fytianos, I. Poulios, Semiconductor-sensitized photodegradation of dichlorvos in water using TiO_2 and ZnO as catalysts, Appl. Catal. B 59 (2005) 81–89.
[26] D.R. Lide, Handbook of Chemistry and Physics, Seventy sixth ed., CRC Press, London, 1995.
[27] K.H. Wang, Y.H. Hsieh, M.Y. Chou, C.Y. Chang, Photocatalytic degradation of 2-chloro and 2-nitrophenol by titanium dioxide suspensions in aqueous solution, Appl. Catal. B 21 (1999) 1–8.
[28] K.I. Ishibashi, A. Fujishima, T. Watanabe, K. Hashimoto, Quantum yields of active oxidative species formed on TiO_2 photocatalyst, J. Photochem. Photobiol. A 134 (2000) 139–142.